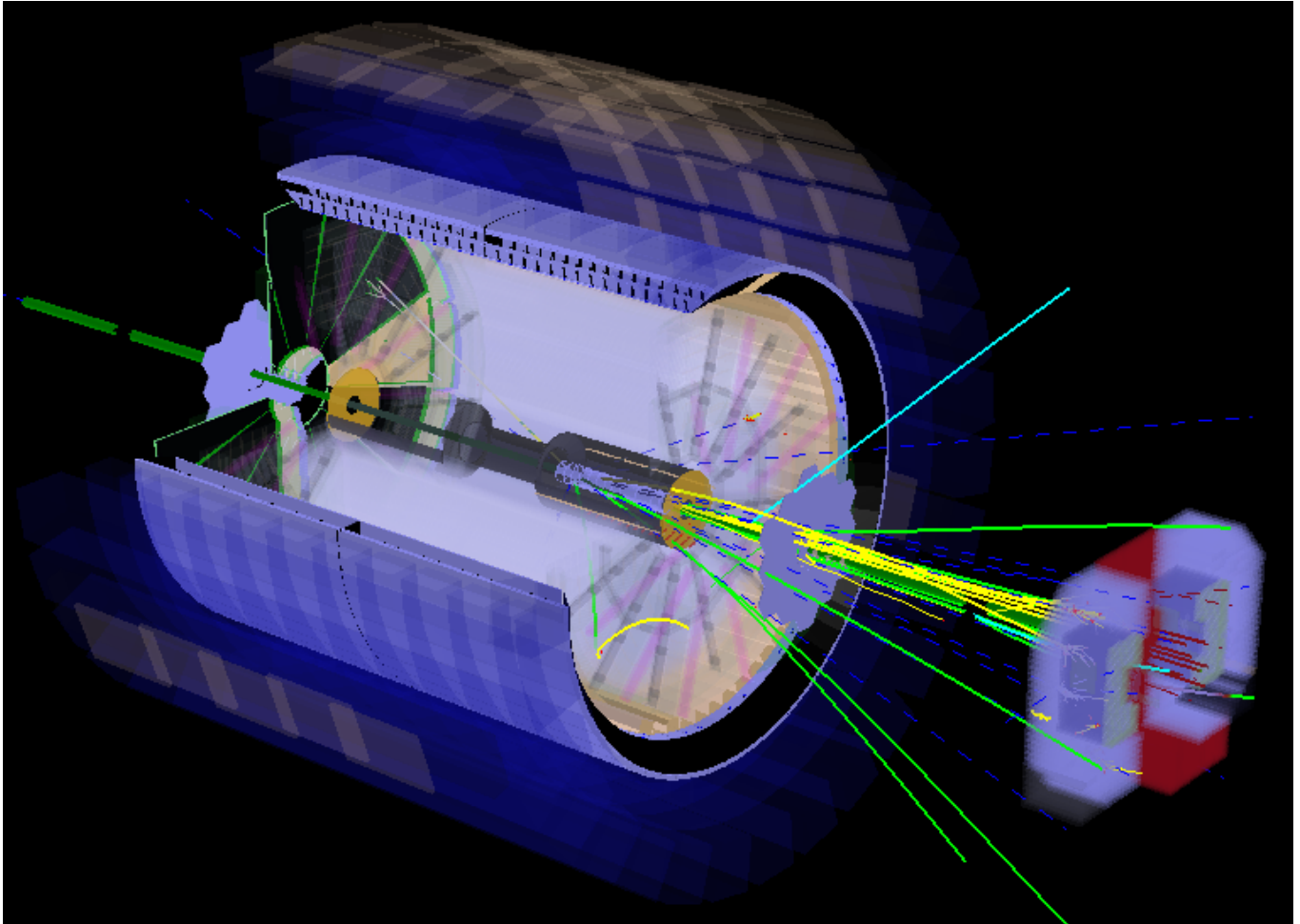


# Physics Opportunities with STAR in 2020+

The STAR Collaboration  
(Dated: October 19, 2015)



## I. INTRODUCTION

The 2015 NSAC Long Range plan notes in the first recommendation that “*the upgraded RHIC facility provides unique capabilities that must be utilized to explore the properties and phases of quark and gluon matter in the high temperatures of the early universe and to explore the spin structure of the proton*”. In this document we outline the STAR collaboration’s plans for the 2020+ era, which are perfectly aligned with this mission. These plans include a suite of unique measurements that can only be made with a  $p+p$ ,  $p+A$ , and Au+Au collider at center-of-mass energies below 500 GeV. They are designed to capitalize on STAR’s existing resources which include a proven multi-purpose detector, established calibration techniques and highly developed software infrastructure. The program outlined here is an essential step towards the completion of the RHIC mission and will provide a natural transition to the highly anticipated electron-ion collider program.

Key physics opportunities envisioned by STAR in 2020+ include:

- Studies of the nuclear parton distribution and fragmentation functions
- Understanding of the nature of the pomeron and potentially discovering the odderon
- Extension of gluon polarization results down to low- $x$
- Constraints on the transport coefficients  $\hat{e}$  and  $\hat{q}$  near  $T_c$ .
- Constraints on the 3+1D hydrodynamic and temperature dependence of QGP properties

The measurements needed to probe these physics questions will require several upgrades to the existing STAR detector. The iTPC and Event Plane Detector, which are planned for the BES-II period, will increase STAR’s mid-rapidity acceptance, event plane resolution, and centrality determination. In addition to these upgrades, STAR proposes to 1) enhance significantly our forward capabilities via a package of highly segmented electromagnetic and hadronic calorimetry and a silicon based tracker, 2) replace the current HFT-PIXEL detector with next generation MAPS sensors and new electronics, and 3) implement new read-out electronics on most detectors, which will allow  $\sim 5$  kHz or higher in Au+Au collisions. These upgrades will allow for qualitative advances in the precision and detail with which RHIC can probe cold nuclear matter and the strongly-coupled QGP, in a cost-effective way that is complementary to sPHENIX at RHIC as well as experiments at the LHC and JLAB.

This document first briefly describes what data STAR plans to have exploited prior to 2021 running. In Section III we explain the assumptions we made for RHIC top energy Au+Au,  $p+p$ , and  $p+A$  running in 2021-2022. In Sections IV and V we describe the key physics observables STAR will contribute in the 2020+ era. Finally, in Section VI, we outline three cost effective upgrades to allow the collaboration to fully participate in the completion of RHIC science mission by continued running in 2020+.

## II. RESULTS ANTICIPATED BY 2020

In the next few years, STAR will make significant progress towards achieving our spin and relativistic heavy-ion physics goals on a timescale consistent with intense international interest and competition in these areas. The following sub-sections outline STAR’s current plans for publications and analyses resulting from the RHIC running up to and including the BES-II.

### A. Spin and Cold QCD

The natural evolution of the RHIC spin and cold QCD program informs the goals of the community in 2020+. Before the turn-on of RHIC in 2000 the flagship measurements were those sensitive to the gluon (HP Milestone 12) and sea quark helicity (HP8) distributions. These campaigns were extremely successful, with the STAR inclusive jet asymmetries [1] indicating that the gluon spin contribution to the spin of the proton may be comparable to the quark spin contribution ( $\sim 25\%$ ) and the W boson asymmetries [2] providing the first clear indication of flavor symmetry breaking in the polarized sea.

The gluon and quark helicity measurements require longitudinally polarized proton collisions, but the versatility of the RHIC facility allows for collisions of transversely polarized protons as well. In fact, the first spin measurement to be published from RHIC was the large neutral pion transverse single spin asymmetry (SSA) in the forward direction at STAR [3]. Significant asymmetries had been measured at lower  $\sqrt{s}$  in fixed target experiments, but STAR was the first to show that these asymmetries persisted at much higher center-of-mass energies, i.e. in the realm of perturbative QCD. Since that seminal measurement STAR has pursued a series of experiments aimed at understanding the mechanism behind these large  $\pi^0$  SSAs. Measurements of photon multiplicities [4] and  $\pi^0$  mesons in forward jets indicate that the source of this asymmetry cannot be dominated by 2-2 scattering in perturbative QCD physics. During the 2015 RHIC run STAR collected a significant sample of diffractive scattering events. These events are characterized by correlating a jet or  $\pi^0$  in the forward meson spectrometer with a proton in the Roman Pot detectors installed around the beamline at IR6. If diffractive events are found to contribute substantially to the  $\pi^0$  single spin asymmetries, it will not only shed light on a decades old mystery, but it will also be the first observation of significant spin asymmetries in diffractive  $p+p$  collisions.

These forward  $\pi^0$  measurements at STAR tapped into a burgeoning world-wide quest to understand the origin and nature of transverse single spin asymmetries, both in  $p+p$  and  $e+p$  DIS collisions, and motivated in part the HP 13 milestone that called for tests of “unique QCD predictions for relations between single-transverse spin phenomena in  $p+p$  scattering and those observed in deep-inelastic lepton scattering.” This rapidly evolving discussion in the spin community motivated STAR to explore completely new measurements, for example mid-rapidity di-hadron [5] and hadron+jet [6][7] SSAs. These asymmetries provided the first ever access to transversity distributions at high  $Q^2$  and insights into potential factorization breaking effects in  $p+p$  collisions. Another example is the SSA of fully reconstructed W bosons at mid-rapidity [8], which STAR plans to measure in the upcoming 2017 run. These asymmetries, combined with the forward inclusive photon SSA, will provide a deep test of the transverse momentum dependent (TMD) framework and its relationship to the well-established collinear QCD framework traditionally used to extract parton distribution and fragmentation functions. Tests of the TMD framework in  $p+p$  collisions are not only essential for the progress of spin physics, but are part of a larger conversation about the role of transverse momentum distributions in QCD, a topic being explored at JLAB, FNAL and CERN.

The data taken in recent years at RHIC, combined with measurements from experiments at the LHC, HERA and Tevatron, should allow the cold-QCD community to address the pressing questions about TMD factorization, evolution and the relationship to collinear factorization in  $p+p$  collisions by the end of this decade. In the process STAR will have refined the tools needed to tackle the most promising physics opportunities during the final stage of RHIC running. The reconstruction of jets and hadron properties within jets will be essential for studies of both polarized and unpolarized fragmentation function measurements in  $p+p$  and  $p+A$ . Likewise, the clean extraction of prompt photon signals at both  $\sqrt{s} = 200$  (run 2015) and 500 GeV (run 2017) will be critical for the future direct photon studies proposed to isolate and constrain nuclear parton distribution functions. At each phase of the RHIC program STAR has delivered unique results, many that have changed our picture of how quarks and gluon interact inside the proton. STAR is prepared to carry this ethic into the next decade.

## B. Hot QCD

The past decade witnessed huge advances in both experimental measurements and theoretical calculations leading to a deeper and broader understanding of QCD matter under extreme conditions. It is now clear that the QGP is a strongly coupled liquid with a viscosity to entropy density ratio close to the theoretical limit. However, it remains elusive how microscopically the collective features of this fluid emerge from the individual quark and gluon interactions. In addition the precise details of the initial state continue to be debated.

The critical point, if it exists, will provide a landmark in the phase diagram of nuclear matter and guide further experimental and theoretical studies of QCD over a wide range of conditions. The discovery of a QCD critical point would constitute a major scientific achievement in heavy-ion physics. The limited event statistics from BES-I have already allowed significant progress to be made toward the goals that were established at the outset of this program. There are clear indications that hadronic interactions dominate at the lower BES energies and several observables associated with the formation of a partonic phase at top RHIC energy show indications of turn-off [9, 10]. The BES-I program made important first measurements necessary for the understanding of critical point and first order phase transition QCD physics [11]. However, only with the iTPC and EPD upgrades, in combination with the higher RHIC luminosities, will precision measurements of these key observables be possible. These set of focused, high-precision, refined measurements, together with concerted theoretical efforts, will allow the BES-II program to fundamentally

enhance our understanding of the phase diagram of QCD matter.

Heavy quarks are much more sensitive than light quarks to the transport coefficients in the medium. Therefore STAR has launched a comprehensive heavy-flavor program with the two newly installed detectors: the Heavy-Flavor Tracker (HFT) for open heavy-flavor measurements and the Muon Telescope Detector (MTD) for quarkonium measurements. By 2016, RHIC will have completed a long Au+Au 200 GeV run to carry out systematic measurements of heavy flavor hadron production. High precision measurements of  $D^0$  spectra and elliptic flow versus centrality in Au+Au collisions at RHIC will be performed from those datasets. First results on the D meson  $R_{AA}$  and  $v_2$  were presented at QM2015 [12, 13]. These results represent the first step in disentangling charm from bottom quark interactions with the QGP at RHIC. They suggest a strong suppression of open charm hadrons and favor models incorporating charm quark diffusion in the medium. The models can currently simultaneously explain both the measured  $R_{AA}$  and  $v_2$  with a diffusion coefficient between 2-10.

Since quarkonia states probe the thermal length scales of the QGP, measurements of the in-medium dissociation probability of the different quarkonium states are expected to provide an estimate of the initial temperature of the system. Dissociation of quarkonium in a thermal QCD system would ultimately provide evidence of color screening and free quarks. High-precision  $J/\Psi$  spectra and elliptic flow in different centrality bins in Au+Au collisions at RHIC will be performed.  $\Upsilon(1S, 2S, 3S)$  states provide a natural thermometer since they are three consecutive mass states of the same species, the 1S state is predicted to not dissociate at RHIC energies which makes it a standard candle, and the effects of bottomonia recombination at RHIC is negligible. Measurement of yield ratios between different states ( $\Upsilon(2S+3S)/\Upsilon(1S)$ ) from the full statistics of the MTD are projected to be within 10% statistical errors. The  $\psi(2S)$  should also be possible and is currently not well measured at RHIC energies. Since it is less tightly bound it should be more suppressed than the  $\Upsilon$  states but, recombination effects might also be present. In combination with the low  $p_T$   $J/\Psi$  results, measurement of the  $\psi(2S)$  would give us deeper insight into the rate of dissociation and recombination. The first quarkonia signals from the MTD with limited statistics were presented at QM2015 [14]. We are aiming for exploratory measurements of the  $\Lambda_c$  baryon as well as bottom hadrons through their decay to  $J/\Psi$ , as well as the semi-leptonic decay channels before 2020, which will inform our analyses of the high statistics running with the enhanced HFT detector and ensure timely publication of the results.

New results shown at DIS [15], HP2015 [16], and QM2015 [17] clearly illustrate STAR's jet capabilities and the power of these tools to add clarity to the study of the QGP, including how the lost energy is dissipated. New di-jet imbalance measurements,  $|A_J|$ , indicate that while the substructures, for a biased set of jets with hard cores, are broadened and softened the majority of the energy is retained within a jet cone radius of  $R=0.4$ , which is very different from measurements at the LHC which indicate significant energy is dissipated far from the jet. Charged jets recoiling from a high- $p_T$  hadron show a larger jet suppression than those at the LHC, but the required energy shift of the spectrum is less. The energy shift is also smaller for larger cone radii, as expected if interactions with the QGP cause a broadening of the jet substructure. These new analyses are consistent with STAR's jet-hadron publication which also indicated a softening and modest broadening of the recoil jet [18]. These results also suggest a coupling to the medium traversed which differs to that at the LHC. The steeply falling jet spectrum at RHIC allows for a tight correlation between the trigger hadron and the initial parton energy. This also allows for geometrical engineering of the average pathlength probes by the measured jet. Finally, new gamma-hadron results [19] show a similar suppression as a function of  $z_T$  when compared to  $\pi^0$ -hadron correlations. These results are in contrast to expectations from models including in-medium shower modifications and energy redistribution within the jet and will provide strong constraints on future modeling of the energy loss.

### III. ASSUMPTIONS FOR RUNNING IN 2020+

We assume two STAR running periods, concurrent with sPHENIX running, after the completion of BES-II. The combined RHIC and STAR uptime is anticipated to be 50%. We further assume that in addition to the current STAR detector suite prior to the BES-II, the Event Plane Detector (EPD) and iTPC will have been installed. By 2021 STAR will also need to have constructed and installed the Forward Upgrades, the HFT+, and increased the DAQ rate of all detectors to enable the full suite of STAR's key physics programs, however many of the measurements can be obtained with nothing but continued running or only one of the proposed upgrades.

Our data estimates are based on the latest RHIC Collider Projections [20] released in April 2015. As for our previous BUR estimates, we take the average of the maximum and minimum projected luminosities assuming a luminosity ramp-up during the first three weeks of the run and 70% running efficiency for STAR. In 2021 we assume 20 weeks

of Au+Au physics running with a luminosity of  $70 \times 10^{26} \text{ cm}^2\text{s}^{-1}$  of which 23% is recorded within  $|z_{vertex}| < 10\text{cm}$ . In the Au+Au streaming mode of data taking, as explained below, STAR will be capable of recording minimum bias events at a rate of  $\sim 5 \text{ kHz}$ , as well as rare triggers. In 2022 we assume that the run is equally divided between  $p+p$  and  $p+A$  running, resulting in 10 weeks of data taking each. The number and type of ion species requested by STAR during the 10 week  $p+A$  period will depend on conclusions drawn from analysis of ongoing  $p+Au$  and  $p+Al$  data taken in the last RHIC run. In  $p+A$   $2.3 \text{ pb}^{-1}$  of data is delivered with  $1.6 \text{ pb}^{-1}$  being recorded. For  $\sqrt{s} = 200 \text{ GeV}$   $p+p$  collisions the expectation is  $270 \text{ pb}^{-1}$  of recorded data. The assumed polarization, is 0.6 (0.55) for 200 (500) GeV  $p+p$  running. Please note these projections differ significantly from those quoted in [21], even before detector efficiency is taken into account.

#### IV. SPIN AND COLD QCD IN 2020+

Existing mid-rapidity detector capabilities combined with a cost-effective forward upgrade will allow STAR to address three broad areas of interest within the spin and cold QCD community in the years following the BES-II. These programs will shed light on the dynamics of low and high  $x$  partons in cold nuclear matter (CNM) and how the fragmentation and hadronization of these partons is modified through interactions within the CNM. Proton structure experiments sensitive to the low  $x$  gluon helicity distribution and polarized diffractive effects are possible. All of these measurements utilize the unique running condition provided by RHIC and cannot be made at any existing collider or accelerator facility.

##### A. The Initial State: Nuclear Parton Distribution Functions

Our current understanding of nuclear parton distribution functions (nPDF) is still very limited. Figure 1 summarizes the current state of the art for nPDF fits in Pb at  $Q^2 = 10 \text{ GeV}^2$  for up flavor sea quarks and gluons. The yellow bands highlight the  $x$  regions currently unconstrained by data. In addition to input at low and high  $x$ , it is essential to collect data over a wide range of  $Q^2$  and for several nuclei as the A-dependence of the nPDFs cannot be predicted from first principles with pQCD.

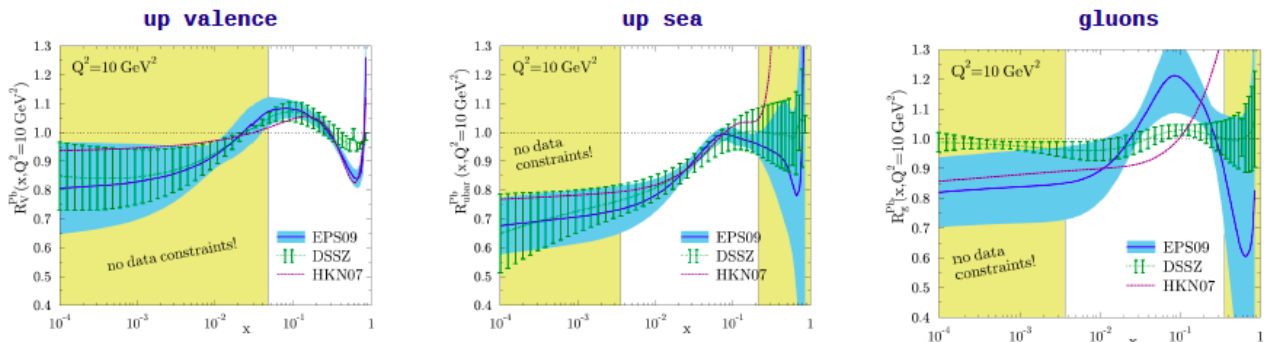


FIG. 1: Up valence quark, up sea quark and gluon nuclear PDFs as referenced in the 2014 DIS talk by H. Paukkunen.

STAR has the opportunity to provide new input to the sea quark nPDFs by collecting Drell-Yan (DY) data with forward instrumentation covering pseudo-rapidities  $2.5 < \eta < 4$ . In addition, direct photon and  $J/\Psi R_{pA}$  will be measured, providing constraints on the gluon distribution in nuclei. Figure 2 shows the kinematic coverage in  $x - Q^2$  of the past, present, and future experiments capable of constraining nPDFs while accessing the parton kinematics event-by-event. All experiments investigate channels which are able to separate strong interactions in the entrance and exit channels in  $p+A$  and  $e + A$  collisions. Note that while some of the LHC experiments do cover the same  $x$ -range as DY at forward pseudo-rapidities at STAR, they only access higher  $Q^2$ , a regime where sensitivity to these nuclear effects is significantly reduced.

The proposed forward calorimeter package will allow direct photon,  $J/\psi \rightarrow e^+e^-$ , and DY measurements. The total DY cross-section is on the order of  $10^{-5} - 10^{-6}$  of the hadron production cross-sections, therefore the probability of mis-identifying a hadron track as  $e^+/e^-$  has to be suppressed down to the order of 0.1% while maintaining reasonable electron detection efficiencies. To that end we have studied the combined electron/hadron discriminating power of the proposed forward tracking and calorimeter systems. It has been shown that by applying multivariate analysis techniques to the features of EM/hadronic shower development and momentum measurements we can achieve hadron

rejection powers of 200 to 2000 for hadrons of 15 GeV to 50 GeV with 80% electron detection efficiency. Figure 3 shows the DY and background signals, along with the associated uncertainties for an integrated luminosity of 500  $pb^{-1}$  in  $\sqrt{s} = 200$  GeV  $p+p$  collisions.

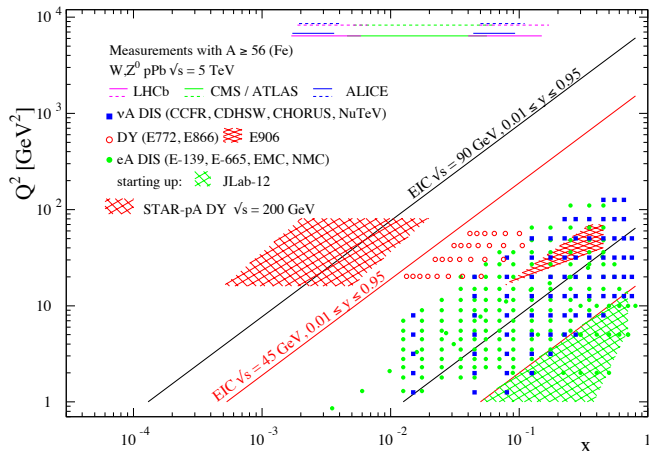


FIG. 2: The  $x - Q^2$  range of past, present, and future experiments capable of constraining nPDFs and have access to parton kinematics event-by-event.

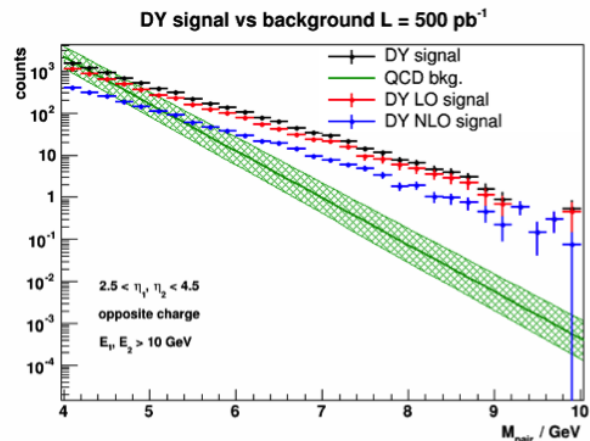


FIG. 3: DY signal and background yield from 500  $pb^{-1}$   $\sqrt{s} = 200$  GeV  $p+p$  collisions.

## B. The Final State: Hadronization in the Nuclear Environment

In spite of the remarkable phenomenological successes of QCD, a quantitative understanding of the hadronization process is still one of the great challenges for the theory. Hadronization describes the transition of a quark or gluon into a final state hadron. It is a poorly understood process even in elementary collisions. RHIC's unique versatility will make it possible to study hadronization in the nuclear medium and with polarized beams.

Data from the HERMES experiment [22][23] have shown that production rates of identified hadrons in semi-inclusive deep inelastic (SIDIS)  $e + A$  scattering differ from those in  $e + p$  scattering. These differences have been explained by a variety of mechanisms ranging from the well-known modification of parton densities in nuclei to interactions between the nuclear medium and the seed partons (before hadronization) or alternatively with the final-state hadrons. Figure 4 shows clearly that the measured multiplicity ratios  $R_{eA}$  for charged and neutral pions as a function of  $z$  for different target nuclei  $A$  cannot be explained using only nPDFs, as nuclear effects of strong interactions in the initial state should cancel in this observable. Only the inclusion of nuclear effects in the hadronization process allows us to reproduce of all the dependencies ( $z$ ,  $x$ , and  $Q_2$ ) of  $R_{eA}$  in SIDIS.

It is critical to see if these hadronization effects in cold nuclear matter persist at the higher  $\sqrt{s}$  and  $Q^2$  accessed at RHIC. Recent theoretical work [27] shows that studying identified hadrons in jets gives us unique access to the hadronization process in  $p+p$  collisions. STAR's excellent jet reconstruction capabilities, paired with its unique ability to identify pions, kaons and protons over a wide momentum range make it the ideal detector to study hadron fragmentation inside jets. Using the 200 GeV  $p+p$  and  $p+A$  data collected in 2015 STAR will be able to make the first measurement of these hadron-jet fragmentation functions. As in the case of the nuclear PDF measurements, it will be critical to collect data with different nuclei to establish the nuclear dependence of possible medium modifications in the final state. The specific nuclei to be studied remains to be determined.

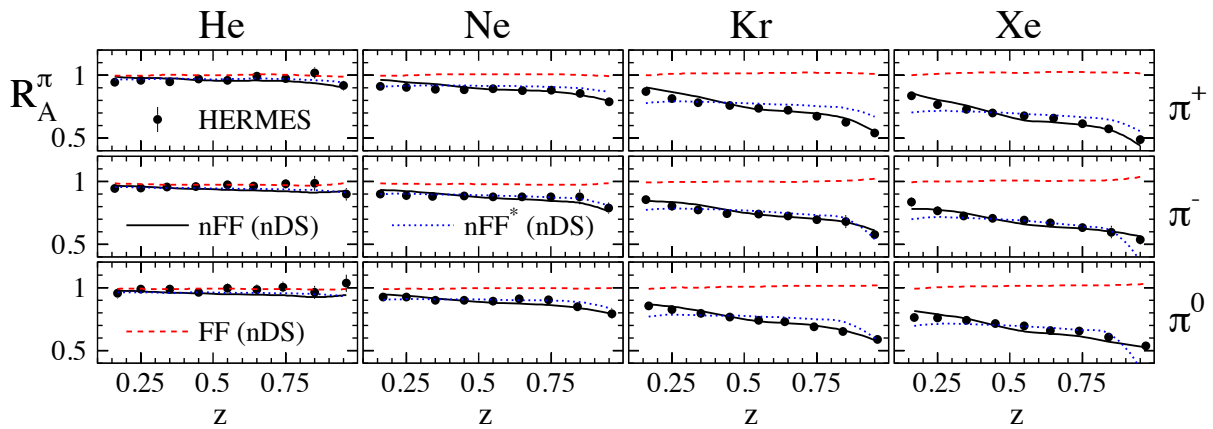


FIG. 4:  $R_{eA}$  in SIDIS for different nuclei in bins of  $z$  as measured by HERMES. The solid lines correspond to the results using both nuclear FFs and the nDS medium modified parton densities[24]. The red dashed lines are estimates assuming the nDS medium modified PDFs but standard DSS vacuum FFs, and indicate that nPDFs are insufficient to explain the data [25] [26].

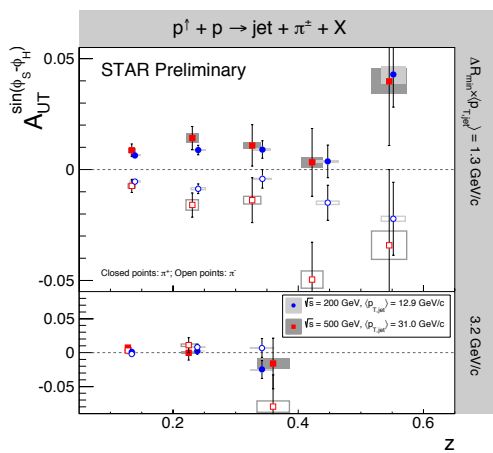


FIG. 5: The first observations of nonzero Collins asymmetries.

RHIC's ability to polarize the colliding proton beams provides the unique opportunity to simultaneously study both nuclear and spin effects in the hadronization process. The Collins fragmentation function,  $H_1^\perp$ , describes the correlation between the transverse spin of a fragmenting quark and the transverse momentum of a given hadron produced during hadronization. In transversely polarized  $p+p$  collisions the probability of finding a transversely polarized quark times the  $H_1^\perp$  function may be accessed through single spin asymmetries of the azimuthal distributions of hadrons inside a high-energy jet. Figure 5 shows the first observations of nonzero Collins asymmetries in  $p+p$  collisions at  $\sqrt{s} = 200$  and 500 GeV by STAR [6][7]. These SSAs depend strongly on  $j_T$ , the momentum of the pion transverse to the jet thrust axis. This effect is demonstrated in the lower panel where the asymmetries are reduced as the hadrons are restricted to larger values of  $j_T$ .

The effect of a nuclear medium on the Collins function has never been explored. STAR has the unique opportunity to be the first and only detector to probe these spin dependent hadronization effects by expanding the existing analysis from  $p+p$  to  $p+A$  collisions. STAR collected a proof-of-principle set of transversely polarized  $p+A$  data during the 2015 run. While this data should provide a first estimate of the size of medium induced effects, a higher statistics polarized  $p+A$  dataset and a scan in  $A$  is essential to precisely determine the mass dependence of these effects.

### C. A First Look at Spin Dependent Diffractive Scattering

At RHIC center-of-mass energies diffractive scattering events constitute  $\sim 25\%$  of the total inelastic  $p+p$  cross-section [28]. Diffraction is defined as an interaction that is mediated by the exchange of the quantum numbers of the vacuum, as shown in Fig. 6. Experimentally these events are characterized by the detection of a very forward scattered proton and jet (singly diffractive) or two jets (doubly diffractive) separated by a large rapidity gap. Central diffraction, where two protons, separated by a rapidity gap, are reconstructed along with a jet at mid-rapidity, are also present but suppressed compared to singly and doubly diffractive events.

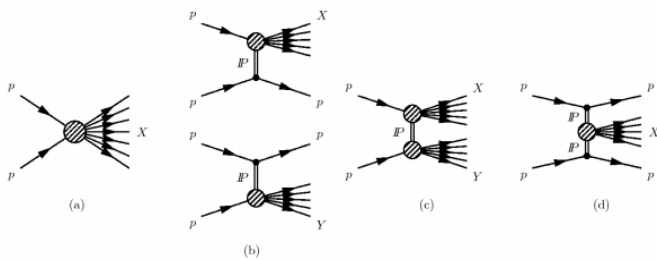


FIG. 6: Schematic diagrams of (a) nondiffractive,  $pp \rightarrow X$ , (b) singly diffractive,  $pp \rightarrow Xp$  or  $pp \rightarrow pY$ , (c) doubly diffractive,  $pp \rightarrow XY$ , and (d) centrally diffracted,  $pp \rightarrow pXp$ , events.

To date, non-diffractive mechanisms have failed to explain the large  $\pi^0$  single spin asymmetries measured by STAR in the forward direction. In 2015 STAR collected data that will permit correlations between forward scattered  $\pi^0$  and tagged protons in its forward Roman Pots. A discovery of large transverse single spin asymmetries in diffractive processes would open a new avenue to study the nature of pomeron exchange in  $p+p$  collisions.

STAR, with RHIC's polarized proton beams, and our Roman Pots (RPs) to tag the forward scattered protons, plus our large jet acceptance  $-1 < \eta < 2$  now and  $-1 < \eta < 4$  after the forward upgrade, will be uniquely equipped to study diffractive phenomena. STAR will be able to measure unpolarized cross sections and single spin asymmetries as a function of pseudo-rapidity at  $\sqrt{s}=200$  GeV. For both observables, the rapidity gap method and the tagging of the forward scattered proton in the STAR RPs can be realized, which will be crucial to constrain calculations on single vs. elastic diffractive cross sections. A non-zero asymmetry would be the first observation of the three gluon / odderon exchange.

#### D. Additional Physics Opportunities at $\sqrt{s} = 500$ GeV

At this time the RHIC plan does not include collisions above  $\sqrt{s} = 200$  GeV in the years after 2020. If the timeline for the proposed EIC should slip, making additional running time feasible, STAR would advocate running  $p+p$  at  $\sqrt{s} = 500$  in order to make a low  $x$  measurement of the gluon helicity distribution  $\Delta g(x)$ . The existing inclusive and di-jet mid-rapidity analyses are sensitive to gluons in the range of  $0.02 < x < 0.5$ . While these measurements clearly point to a positive  $\Delta g(x)$  for moderate  $x$  values, they do little to constrain the functional form of the distribution at lower  $x$ . This lack of data translates directly into a large uncertainty on the total gluon contribution to the spin of the proton  $\Delta G = \int_0^1 \Delta g(x)$ . It is possible to access regions of  $x \sim 10^{-3}$  by pushing di-jet reconstruction into the forward region at STAR. Jet reconstruction in the forward region, i.e.  $2.5 < \eta < 4.0$ , will require electromagnetic and hadronic calorimetry as well as tracking to allow association of charged particles with a single vertex. Figure 7 shows the  $x$  coverage for four topological di-jet configurations as determined using NLO [29] calculations. EAST, WEST and EEMC refer to the reconstruction of one of the di-jet pair in an existing electromagnetic calorimeter located at  $-1 < \eta < 0$ ,  $0 < \eta < 1$  and  $1 < \eta < 2$  respectively. FCS refers to the forward upgrade package. Figure 8 shows the projected di-jet  $A_{LL}$  statistical and systematic errors for each topological region, compared to the NLO calculations [29]. An uncertainty  $5 \times 10^{-4}$  has been assumed for the systematic uncertainty due to relative luminosity. A beam polarization of 55% and a total delivered luminosity of  $1 \text{ fb}^{-1}$  have been assumed with a ratio of 2/3 for the ratio of recorded to delivered luminosity.

Collisions of transversely polarized  $p+p$  beams at  $\sqrt{s} = 500$  GeV would also allow STAR to push existing jet+hadron SSA measurements into a new kinematic regime. As discussed in the previous section, jet+hadron SSAs are sensitive to the poorly constrained transversity distributions which describe the probability of finding a transversely polarized quark inside a transversely polarized proton. Forward jet reconstruction provides access to the high quark momentum fractions, up to  $x \sim 0.6$ . Measurements aimed to access this high  $x$  regime will also be pursued during the JLAB 12 GeV program, but at much lower values of  $Q^2$ . As with the low  $x$  gluon helicity program, these jet+hadron SSA observables will rely on the electromagnetic and hadronic calorimetry plus tracking for full jet reconstruction and charged sign discrimination for the hadrons. Although the forward upgrade package does not include particle ID capabilities the tracking is intended to provide charge sign separation. Inclusive  $h^+/h^-$  samples are difficult to interpret because of the undetermined mix of pion, kaons and protons in the sample. However, the low probability of producing a  $K^-$  or  $\bar{p}$  in this kinematic regime should result in a negatively charged hadron sample composed primarily of  $\pi^-$  mesons.

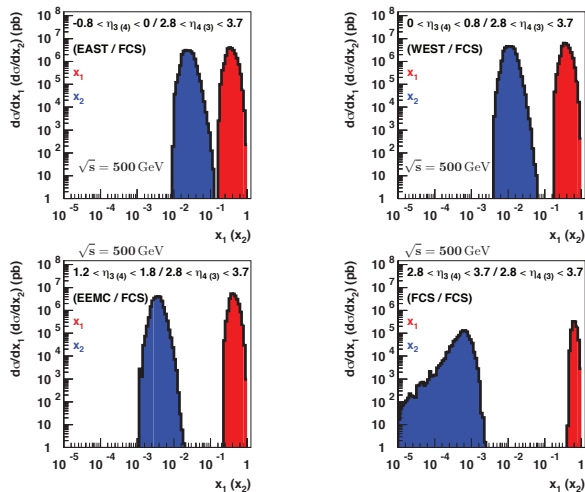


FIG. 7: NLO calculations [29] of the  $x$  coverage for four different topological configurations of di-jets. See text and [30] for details.

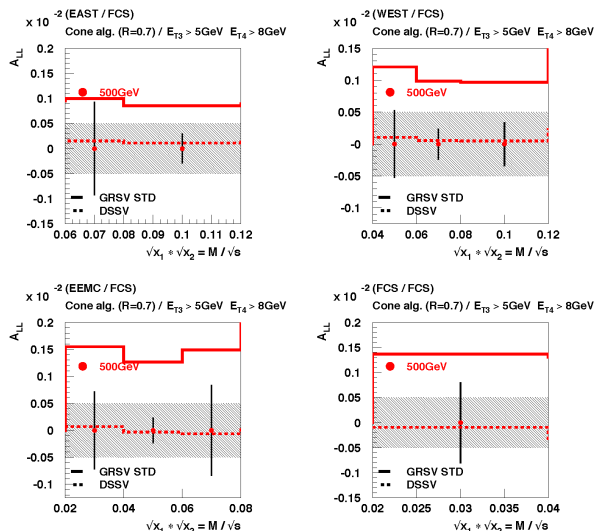


FIG. 8:  $A_{LL}$  NLO calculations as a function of  $\frac{M}{\sqrt{s}}$  for  $2.8 < \eta < 3.7$  together with projected statistical and systematic uncertainties.

## V. HEAVY IONS IN 2020+

An increasingly quantitative description the evolution of the QGP has emerged over the past decade by combining the results of RHIC and the LHC in conjunction with significant improvements in the theory. However, much information about the precise nature of the initial conditions, and how the QGPs properties manifest from individual quark and gluon interactions remains elusive. A key goal of the heavy-ion program in the post-BES-II era is therefore to probe the liquid QGP at varying length scales and to quantify its hydrodynamic properties by mapping its 3+1D expansion. We plan to achieve this goal by utilizing the products of the initial hard scatterings to resolve the medium's properties at increasingly shorter scales and by measuring correlations across a wide rapidity range. By varying the probe momentum and virtuality, we aim to determine the length scale at which the QGP transforms into a strongly interacting liquid formed from its weakly coupled quark and gluon constituents. The longitudinal drag and transverse diffusion experienced by a parton propagating through the QGP are quantified by the leading transport coefficients  $\hat{e}$  and  $\hat{q}$ . By studying in detail the suppression and fragmentation modifications of jets and heavy flavor particles we will provide key data with which to explore the dynamics of the jet-medium interaction in unprecedented detail.

### A. Open Beauty

Comparison of models to the heavily suppressed  $R_{AA}$  and strong azimuthal parameter  $v_2$  of the non-photonic lepton data suggest that heavy quarks, (c- and b-quarks) interact strongly with the hot and dense medium. Since they are heavy compared to u-, d-, and s-quarks, and their masses are not affected by the medium, they serve as clean tools for studying the properties of the medium. At the recent QM2015 conference, new results on identified D-mesons, from both RHIC and LHC energies, have shown collectivity  $v_2$  and suppression of  $R_{AA}$  similar to that of light-quark hadrons. In order to understand these observations and extract information on medium properties, transport coefficients  $\hat{e}$  and  $\hat{q}$ , one must analyze the charm- and bottom-hadron distributions separately. At RHIC, the bottom-hadrons are especially clean probes as they are not affected by the final state interactions, such as recombinations. Figure 9 shows simulations of the expected statistical error on the nuclear modification factor  $R_{AA}$  for non-prompt  $J/\psi$  [Fig. 9 (a)] and  $D^0$ s [Fig. 9 (b)] resulting from the decay of beauty hadrons. With the faster HFT+ and the integrated luminosity of  $10 \text{ nb}^{-1}$  for the top 0-10% 200 GeV Au+Au collisions and  $60 \text{ pb}^{-1}$  for  $p+p$  collisions,  $R_{AA}$  of the beauty hadrons via the  $J/\psi$  is possible, while the beauty decay  $D^0$  and electrons can be measured with reasonable precision up to  $p_T \sim 15 \text{ GeV}/c$ . The  $R_{AA}$  of beauty tagged jets, see the jet section below for further details, can be determined up to  $p_T \sim 40 \text{ GeV}/c$ . Such comprehensive studies will offer us much improved systematic control necessary for a precision understanding of beauty production and modifications by the QGP.

Preliminary measurements at the LHC indicate that charm quarks are thermalized at LHC energies, with flow as large as that of the light flavor hadrons. On the contrary, charm quarks gain significant flow from diffusion in the medium at RHIC energies without complete thermalization. It is therefore important to study beauty quark thermalization at RHIC and the LHC to further elaborate on the temperature dependence of the QGP's properties and heavy-quark diffusion coefficient. Results from  $R_{AA}$  at the LHC suggest a significant energy loss hierarchy on parton mass, but it is less evident at RHIC energies in part due to lack of precision data on whether the jets originated from gluon, light-, charm-, or beauty-quarks. Beauty jet measurements at the relevant jet energy at RHIC and the LHC will help us pin down the dominant energy loss mechanism. The proposed heavy-flavor program is a significant step forward from the present RHIC program based on the HFT project and are complementary to the heavy-flavor program at the LHC

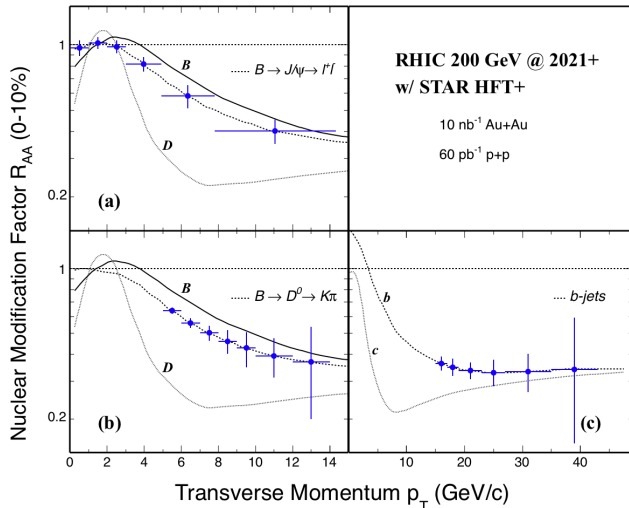


FIG. 9: Statistical error projection for  $R_{AA}$  in 0-10% Au+Au 200 GeV collisions for (a)  $J/\Psi$ s, (b)  $D^0$ s from beauty decays and (c) b-tagged jets with data collected by the HFT+. The  $R_{AA}$  curves for B/D hadrons and b/c quarks are from theory model calculations from TAMU, Duke, and CUJET3.0 [31–33].

The preliminary results from the HFT presented at QM2015 on  $D^0$  elliptic flow [13] strongly enforce that charm quarks couple strongly to the expanding medium. These results necessitate the investigation of the potential flow of beauty quarks. The precision  $R_{AA}$  measurements of bottom hadrons enabled by HFT+ alone and shown in Fig. 9, combined with the precision knowledge on charm hadron  $R_{AA}$  and  $v_2$ , will offer insights into the flavor dependence of heavy quark diffusion in the QGP medium [34]. Measurements of bottom elliptic flow remain challenging and would require a significantly larger data sample than for the  $R_{AA}$  measurements. Such a large statistical sample could be provided with an improved TPC DAQ rate and implementation of the streaming readout.

## B. Jets

Jets, by probing sub-thermal scales, will potentially allow us to determine the length scale at which the QGP's discrete scattering centers dissolve into a collective, continuous medium. Given the expected increased luminosity of  $70 \times 10^{26} \text{ cm}^2 \text{ s}^{-1}$  during Au+Au running our kinematical reach and statistical precision for jet reconstruction will be significantly enhanced. For fully reconstructed jets, the  $p_T$  reach will be extended to 70 GeV with no to little bias in the most central events. This will allow for detailed exploration of not only modifications of the partonic fragmentation into hadrons, including particle identification, but also potential modifications to the back-to-back jet scattering distributions, as well as modifications of the intra-jet angular structure. As shown in Fig. 10, by utilizing various jet trigger types, jet-finding parameters, and kinematic cuts, we can implement jet geometry engineering to bias jet production points, path lengths and interaction probabilities within the colored medium [35]. For instance, since photons are colorless, and hence non-interacting with the QGP, they provide the energy of the recoiling hard scattered parton. Therefore direct photons are a promising unbiased trigger to probe average partonic energy loss, as shown in Fig. 10 bottom left. By studying features of jet produced by the recoiling quark we can directly probe *quark* energy loss. Next-to-leading order pQCD calculations show that surface and volume emissions of this recoiling quark are dominated at large and small  $z_t$  respectively [36].

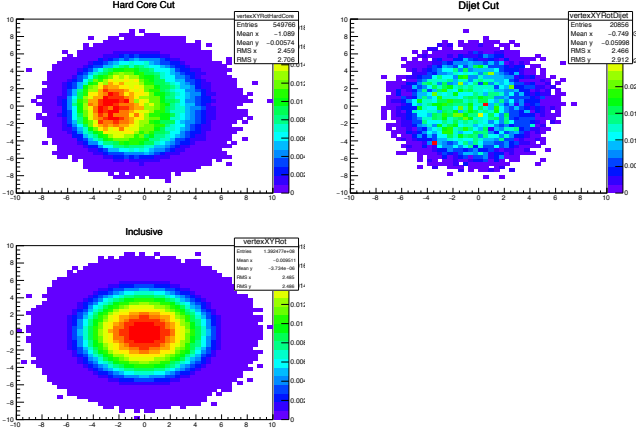


FIG. 10: The production vertex distributions for various jet selections as predicted by JEWEL for 200 GeV Au+Au collisions [37]. Jets are always propagating along the  $-x$  direction. Top Left: Jets with at least one constituent with  $p_T > 6$  GeV/c. Top Right: Di-jets with a leading jet with  $p_T > 20$  GeV/c from constituents over 2 GeV/c and an opposing ( $\Delta\phi > 2\pi/3$ ) sub-leading jet with  $p_T > 10$  GeV/c from constituents over 2 GeV/c. Bottom Left: All jet vertices generated.

Hadron-jet correlations allow detailed exploration of the recoil jet with no bias imposed on the recoil jet's fragmentation. As shown in Fig. 10 the high- $p_T$  trigger hadron imposes a surface bias, resulting in the recoil jet traversing a longer than average path-length. Figure 11 shows the preliminary h-jet results presented at QM2015 [17] and the expected statistical precision resulting from the 2020+ era. The grey band represent the current statistical and systematic uncertainties while the red bands are those expected from 1B central and 2B peripheral Au+Au events. As noted above, the preliminary results show a strong suppression of the recoil jet even with  $R=0.5$ . A significant improvement in both the systematic uncertainties and the reach in  $p_T$  will be obtained by running in 2020+, in addition the analysis will be extended to full jets. With this improved precision, we can explore over a wide range of jet energies and trigger hadron  $p_T$  the energy loss and redistribution of these recoil jets.

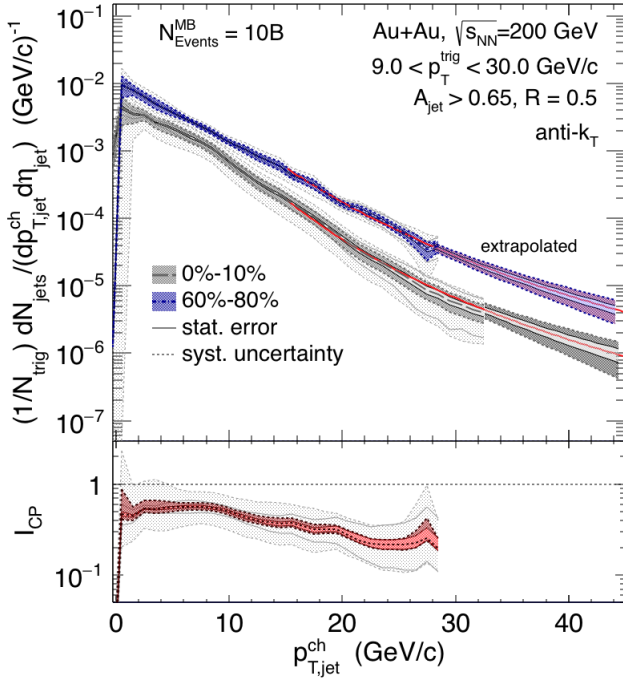


FIG. 11: Present and projected h-jet  $I_{CP}$  from measurements of central and peripheral Au+Au events with  $R=0.5$ . A constant suppression of the recoil jet is assumed in the projections.

Jet virtuality has a considerable effect on fragmentation functions and other jet shape observables. Experimentally the virtuality evolution can be accessed by measuring the mass of the jet [38], adding a new dimension to jet quenching measurements. By constraining both of the relevant quantities, energy and virtuality, and is expected to provide non-trivial tests for models of in-medium shower evolution in heavy-ion collisions, in particular if contrasted with complementary LHC measurements. With the increased statistics in 2015 and beyond, STAR can perform a first measurement of jet mass at RHIC energies.

In the weak coupling limit it has been conjectured that the large  $\Delta\phi$  region is dominated by single hard Molière scatterings as the point-like particulate nature of the QGP is resolved by the jet [39]. Initial explorations for evidence of large angle scattering of the recoil jet were reported at QM2015 [17]. These preliminary studies utilized charged jets on the recoil side to a high  $p_T$  charged hadron; clearly more statistics are required before any firm conclusions can be drawn. However the analysis and the background are controlled. RHIC is ideal for such explorations since vacuum QCD effects, those that lead to 3-jet events for instance, fall off rapidly, meaning background at large  $\Delta\phi$  should be minimal. This is currently an

active area of theoretical study and more detailed calculations of the size of the signal are currently underway which will allow us to make an estimation of the required sampled luminosity.

By utilizing the HFT+ STAR will also be able to study b-tagged jets (i.e. jets resulting from a scattered b quark). These measurements are of particular importance to fully understand the energy loss mechanisms of these heavy quarks since they are predicted to have different sensitivities to collisional and radiative energy loss mechanisms compared to light quarks and gluons.

Indeed the non-photonic electron results from RHIC indicate that radiative energy loss models do not predict the observed suppression. Our expected performance for measuring the  $R_{AA}$  for b-tagged jets is shown in Fig. 9 (c). The sub-structure of these jets can also be studied to determine how the lost energy re-emerges, and if this energy redistribution is as broad and at as low  $p_T$  as that observed via our light flavor jet correlation measurements.

With charged particles from the TPC and full EMCal coverage, we can fully reconstruct jets as demonstrated with published or preliminary results from  $p+p$ ,  $p+A$ , and Au+Au results. STAR utilizes the anti- $k_T$  jet finding algorithm [40, 41]. Correction procedures for unmeasured particles, detector effects, and fluctuating backgrounds in heavy ion collisions which have been developed over the past decade, first at RHIC and then perfected at the LHC, have been adopted to STAR. In addition the factor 2 increase in  $\eta$  acceptance due to the iTPC will be utilized to perform charged jet analyses. The viability of this procedure has been demonstrated in preliminary results from STAR and publications by both ALICE and CMS.

STAR's EMCal, with a resolutions of  $\sigma/\sqrt{E} = 15\%$ , has a  $0.05 \times 0.05$  segmentation. This segmentation means it is highly probable for the decay photons of a 15 GeV  $\pi^0$  to be recorded in the same tower. However, as has been demonstrated in the STAR direct photon-hadron correlations [19, 42], STAR can utilize the transverse shower profile (TSP) to help discriminate at these energies even in Au+Au data. While above  $p_T \sim 25$  GeV this technique no longer works, the  $\pi^0$  is so strongly suppressed in central Au+Au data that the  $\gamma/\pi^0$  ratio exceeds 1 for  $p_T > 20$  GeV/c. In addition, at these high  $p_T$  one can implement isolation cuts, requiring the absence of nearby mid- to high- $p_T$  charged tracks to distinguish direct photon from  $\pi^0$  triggers. The expected luminosities in the 2020+ era translate into  $\sim 2500$  direct photons with  $p_T > 30$  GeV in the most central collisions.

### C. Longitudinal Correlation Studies

Correlations from flow, in particular their event-by-event fluctuations, have been a crucial tool for understanding the space-time picture of heavy-ion collisions and the properties of the QGP phase. However, event-by-event QGP dynamics in the longitudinal directions remain poorly understood. Such studies are vital to adequately constrain the current suite of sophisticated theoretical frameworks that incorporate not only realistic initial conditions and the interactions of hard processes with the medium, but also 3+1 viscous hydrodynamics coupled to hadronic transport codes. In addition to uncertainties in the initial state, uncertainties remain in the physics of the hydrodynamic models themselves that need to be addressed. Correlations induced by thermal fluctuations or mini-jets can also introduce uncertainty in the value of  $\eta/s$  extracted from correlation functions measured in heavy-ion collisions [43]. By mimicking viscous effects these correlations can lead to an overestimate of the actual viscosity. The most promising experimental method to estimate their contribution is to measure the pseudo-rapidity dependence of correlation functions.

New flow observables, that help further elucidate the space-time picture of the QGP evolution in both the transverse and longitudinal directions, will be enabled by our forward upgrade program. These novel measurements will enhance our understanding of QGP at 200 GeV and provide a crucial step towards completion of the mission of the RHIC heavy-ion program. Active theory and experimental explorations of new measurements in longitudinal correlations have produced several promising tools in probing initial sources, nuclear stopping, longitudinal pressure/flow, and hydrodynamic fluctuations throughout the evolution. Examples of these proposed measurements are: mixed harmonic correlations of reaction planes, torque (twist) of event shape, the Legendre coefficients of the two-particle pseudo-rapidity correlation functions [44–46] and Principal Component Analyses [47, 48]. In combination with similar measurements at the LHC, and the existing large set of published data on the event-averaged flow, they will also provide necessary constraints on the temperature evolution of the QGP properties.

Calculations of the number of participating nucleons,  $N_{part}$ , and the associated eccentricity vector,  $\epsilon_n = \epsilon_n e^{in\psi_n}$ , separately for the forward-going and backward-going nuclei, show that  $N_{part}^F \neq N_{part}^B$  and  $\epsilon_n^F \neq \epsilon_n^B$  in most events. This suggests that in a single event the entropy production, and the shape of its transverse profile, at early times could exhibit a large forward-backward (FB) asymmetry and twist. These initial fluctuations result in signals that survive the medium's expansion and appear in the final state as a FB asymmetry in the particle multiplicity ( $dN/d\eta(\eta) \neq dN/d\eta(-\eta)$ ) and  $v_n(v_n(\eta) \neq v_n(-\eta))$ , as well as FB-twist of the observed event plane angles  $[\phi_n(\eta) - \phi_n(-\eta)]$ .

Measurements of the  $\eta$  dependence of the multiplicity fluctuations and event plane decorrelations therefore directly probe the initial state and early time dynamics of the QGP. These results will also serve as critical constraints to the full 3+1D event-by-event viscous hydrodynamic models that are currently under development. If these FB fluctuations and decorrelations are ignored, our understanding of the temperature dependence of  $\eta/s$  will be, at best, incomplete, as initial measurements at LHC suggest these effects are quite significant [49]. Figure 12 shows measurements of the event plane decorrelations and comparison to the hydrodynamic simulation from CMS [50]. In comparison to the LHC, RHIC has a more compressed rapidity window, this is predicted to result in stronger FB signals. Based on the LHC results it is therefore critical to measure and interpret such signals, and their effects on the medium's evolution, at RHIC. Our forward upgrade program will provide a unique ability to accurately determine  $\eta/s$  at its minimum near the phase boundary. However, the present RHIC results have limited sensitivity due to low statistics and large systematical uncertainty from detector non-uniformity in the forward rapidity. These comparisons show the importance of datasets with high statistics and detector uniformity at forward rapidity with fine granularity.

In the transverse direction, current state-of-art flow correlation measurements are focused on a large class of new multi-harmonic observables, which are sensitive to higher-order eccentricity fluctuations in the initial state and mode-mixing effects in the final state evolution. The interplay between these two contributions leads to non-trivial correlations between multiple event planes of different order. Many such event plane correlators have been measured at the LHC [51, 52], and have been shown to be sensitive to the nature of the initial density fluctuations and dynamics of the collective evolution, as well as the EOS and temperature dependence of the  $\eta/s$ . Measurements of these observables at RHIC at mid- and forward-rapidities, and, very importantly, as a function of  $p_T$ , are expected to provide strong constraints on the space-time picture and medium properties at lower temperatures. These measurements require correlations of the flow signal in several non-overlapping pseudo-rapidity windows. The limited detector coverage of STAR and PHENIX currently prevent such studies at RHIC but the forward upgrade program will provide such capabilities. Construction of correlations between mid-rapidity and forward rapidity can be performed with an event plane detector (EPD) with fine granularity. However, experiments at the LHC (ATLAS and CMS) have shown the importance, and power, of using energy flow from forward calorimetry to construct correlations at forward rapidity. Forward tracking and calorimetry provide the necessary energy and momentum measurements at the different rapidities used for these novel correlation functions.

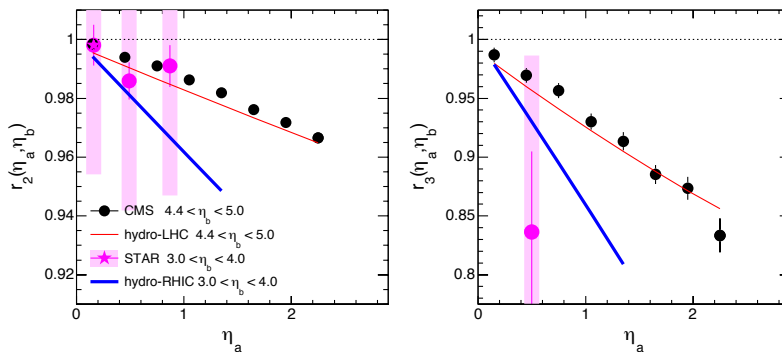


FIG. 12: The comparison of the decorrelation of  $v_2$  (left panel) and  $v_3$  (right panel) between  $\eta_a$  and  $\eta_{-a}$  with reference detector chosen at certain  $\eta_b$  range between CMS data (black circles), STAR data (purple circles), and hydrodynamic model calculations for LHC (thin lines) and RHIC (thick lines) energies. The correlator  $r_n$  is calculated from the two-particle flow coefficients  $V_{n\Delta}$  as:  $r_n(\eta_a, \eta_b) = V_{n\Delta}(-\eta_a, \eta_b)/V_{n\Delta}(\eta_a, \eta_b)$ . The model describes the CMS data and predicts a much stronger effect at RHIC even with the smaller  $\eta$  range. The large uncertainty of the STAR measurement is due to limitations in the available statistics and detector performance.

#### D. Other Physics Analyses Enhanced by Only Continued Running

$J/\Psi$  suppression due to color Debye screening was one of the earliest proposed QGP signatures, and while this measurement was confirmed, the number of surprises and continuing puzzles when measuring heavy quarkonia have made it a rich field of study in hadron colliders. The recent  $J/\Psi$  measurements from RHIC and the LHC can be described consistently by model calculations incorporating color screening and recombination features. However, quarkonium suppression has been observed in  $p+A$  collisions, indicating that cold nuclear matter effects play a large

role in the observed suppression in heavy ion collisions. Additionally, recombination of the heavy quark pairs in heavy ion collisions indicates that the different processes in hot QCD need to be fully quantified for a full understanding. The  $\Upsilon(1S+2S+3S)$  states are key, as beauty recombination is negligible at RHIC energies. Additionally, there should be no Debye screening of the  $\Upsilon(1S)$  based on Lattice QCD calculations [53], though CNM effects could still play a role, which makes it a standard candle for heavy-ion collisions. The low cross-section for beauty production means that  $\Upsilon$  studies have been severely statistics limited at RHIC, they will benefit immensely from the enhanced statistics from continued running of STAR. The MTD is key to measure different Upsilon states.

The iTPC upgrade will reduce the systematic uncertainties on dielectron excess yield measurements by a factor of two. In addition, the iTPC will extend the acceptance for low-momentum electrons from  $p_T > 0.2$  to  $p_T > 0.1$  GeV/c. This improves the acceptance for dielectron measurement by more than a factor of 2 in the low mass region ( $0.4 < \text{mass} < 0.7$  GeV), and lowers the statistical uncertainties as well. These improvements will enable STAR to have a precise measurement of dielectron excess invariant spectrum in 200 GeV Au+Au collisions. Precise input in the region of small baryon chemical potential, where Lattice QCD calculations are reliable, is critical to link dilepton measurements to chiral symmetry restoration.

The 50% increase of the rapidity acceptance due to the iTPC, plus particle identification, will provide unique possibilities related to chiral magnetic analyses. Data analyses related to the possible chiral magnetic effect (CME) and chiral magnetic wave (CMW) are unique to STAR at RHIC, and further systematic checks are especially required to rule out possible background effects. For example, the differential measurements of the  $\gamma$  correlator vs  $\Delta\eta$  can be extended to higher  $\Delta\eta$  to better determine where the signal disappears.

## VI. PLANNED UPGRADES

To enable the entire program envisioned above to be completed three cost effective upgrades are proposed by STAR and briefly outlined below. In concert they provide unique opportunity for STAR to complement the sPHENIX program as the RHIC mission nears completion.

### A. Forward Upgrade

STAR's forward physics plans call for forward electromagnetic and hadronic calorimetry (FCS) as well as tracking (FTS), primarily to distinguish charge-sign. The design of the FCS is a follow up development of the original proposal presented in the STAR decadal plan and the  $p+p$  and  $p+A$  letter of intent. The goal is to create a cost effective upgrade that allows a natural evolution of the STAR scientific program as RHIC, and the community, advances towards the EIC.

The FCS will have superior detection capabilities for neutral pions, photons, electrons, jets, and leading hadrons in the pseudo-rapidity range of  $2.5 < \eta < 4$ . The reduction in the cost for the FCS is achieved by replacing the originally proposed W/ScFi SPACAL ECal with the refurbished PHENIX sampling ECal. The FCS will also utilize the existing Forward Preshower Detector ( $2.5 < \eta < 4$ ) operated in STAR since 2015. The proposed FCS system will have very good ( $\sim 8\%\sqrt{E}$ ) electromagnetic and ( $\sim 70\%/\sqrt{E}$ ) hadronic energy resolutions. The FCS consists of 2000 of the 15552 existing PHENIX EMCAL towers and 480 HCal towers covering an area of approximately 3 m x 2 m. The hadronic calorimeter is a sandwich lead scintillator plate sampling type, based on the extensive STAR Forward Upgrade and EIC Calorimeter Consortium R&Ds[54]. Both calorimeters will share the same cost effective readout electronics and APDs as photo-sensors. It can operate without shielding in a magnetic field and in a high radiation environment. By design the system is scalable and easily re-configurable. Integration into STAR will require minimal modification of existing infrastructure. The estimated cost of the hadronic and electromagnetic calorimetry is  $\sim$ \$2M.

The FTS is envisioned to consist of four planes of silicon strip detectors with 12 wedges each, providing sign discrimination for charged hadron and coarse vertex reconstruction along the beam direction. The latter will enable STAR to delineate tracks originating from different interactions within the same bunch crossing. This capability will be essential for jet reconstruction in the forward direction. FTS occupancy in most central top energy A+A collisions is estimated to be below 10% at the most forward pseudo-rapidities. The FTS will make use of existing cone infrastructure and is estimated to cost  $\sim 4M\$$ .

## B. HFT+

The current pixel detector, the inner layers of the HFT, will be replaced by state-of-art MAPS pixels, which will allow the HFT to take full advantage of the high luminosity provided by RHIC in 2020+. These new chips are being developed by both CERN and IPHC, and one of the designs will be used for ALICE ITS upgrade which is planned for installation by the end of 2019. The existing HFT infrastructure, including the carbon fiber structure, the air-cooling and the IST outer layer detectors will be reused where possible to reduce costs.

With this upgrade the pixel integration time will be  $\tau_{int} = 30 \mu s$ , a more than factor 6 decrease on the current  $\tau_{int} = 186 \mu s$ . This much shorter integration time significantly reduces the background pileup hits on the pixel detector. An additional advantage of the next generation of MAPS sensors is that they have a much better radiation tolerance which will allow for improved operation in the high 2020+ RHIC luminosities.

Figure 13 shows the single pion track efficiency for HFT systems with different PXL integration times at a ZDC coincidence rate of 100k Hz. The upgrade HFT+ system with an integration time better than  $40 \mu s$  will have a significant increase in tracking efficiency, for example 50% (18%) increase for 0.5 (2) GeV/c pions.

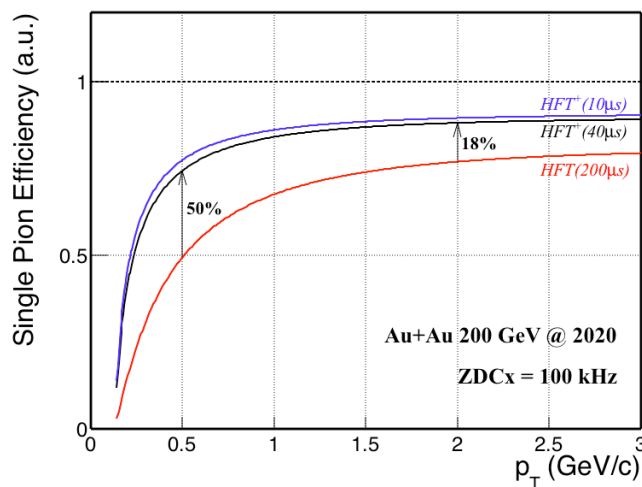


FIG. 13: Single pion efficiency for HFT systems with different PXL integration times of 200(red), 40(black), 10(blue)  $\mu s$  respectively at a ZDC coincidence rate of 100k Hz.

The cost of the HFT+ is estimated at  $\sim$ \$5M.

## C. Limited Streaming Capabilities

In the limited streaming mode the STAR detectors, including the TPC, will be able to stream  $50 \mu s$  worth of collisions at least every millisecond, or 5% of the time (luminosity). For the 100 kHz typical for minimum bias Au+Au collisions this results in  $\sim$ 10 times more data than our current rates, or 5 kHz of Au+Au minimum bias events. This enhanced data taking rate is feasible without any impact on the TPC or its DAQ, no impact on trigger, little impact on tape and DAQ throughput and can be done with already planned upgrades to many important detectors. STAR is also currently exploring options to double the throughput of the DAQ, however even without this improvement STAR could achieve the goals described above.

Due to the necessity to fully drift the whole triggered event, the TPC by nature records for 360 RHIC clocks ( $\sim$ 36  $\mu s$ ). During this time the TPC will also sample ensuing pileup events. If instead of reading for only 36  $\mu s$  we stream for 86  $\mu s$  (i.e. an extra 50  $\mu s$ ) we can sample *and fully read-out* both the triggered event (whose drift time ends at  $\sim$  36  $\mu s$ , as usual) and an additional 50  $\mu s$  of complete future events with the last full events drift time ending at 86  $\mu s$ ). The run configuration would trigger only on rare events at our usual trigger rate of  $\sim$ 1.1 kHz and the minimum bias data would constitute the extra 500 time samples.

While this does increase the data load to DAQ and the charge flowing into the TPC MWPC, this is equivalent to running the TPC at 2-2.2 kHz which is something we think can easily be done as we routinely run at 1.8 kHz.

Operating in this mode would allow STAR to record both 1kHz of rare triggers *while simultaneously* recording  $\sim 5$ kHz of Au+Au minimum bias data:

- with the current TPC gating grid
- with the same anode currents
- with the same DAQ throughput
- with the Trigger system running at only 1 kHz
- with the same amount of data to tape

Depending on the scenarios with the TPC as well as the complement of required detectors we believe that a significantly enhanced DAQ rate is attainable with a budget of  $\sim \$2$ - $3$ M. It should be noted that this cost does not include an estimate for the additional CPU and disk space that would be required to store and analyze this data in a timely fashion.

## VII. SUMMARY

A summary of the connections between STAR's key physics objectives in 2020+, as laid out in Sections IV and V , and the required upgrades, outlined in Section VI, is given in Table I.

Physics Goal	Measurements		Requirements						
			Base	fCal	fTS	RP	HFT+	BSMD	Streaming
<b>Nuclear PDFs</b>	DY, Direct photons +J/Psi R <sub>PA</sub>	★ ■	✓	✓	Enh				
<b>Nuclear FF</b>	Hadron + Jet	★ ■	✓						Enh
<b>Polarized Nuclear FF</b>	Hadron + Jet	★	✓						
<b>Odderon &amp; Polarized Diffraction</b>	A <sub>UT</sub> of pion + forward proton	★		✓		✓			
<b>Low-x ΔG</b>	Di-jets	★	Enh	✓	✓				
<b>High-x Transversity</b>	Hadron+jet	★ ■		✓	✓				
<b>Mapping the Initial State in 3-D: QGP Transport Properties</b>	R. Plane Rapidity de-correlations	★	Needs iTPC						
	Ridge  Δη <3	★	Needs iTPC						
	Ridge  Δη <6	★	Needs iTPC		✓				
	Forward Energy Flow	★	Needs iTPC	✓					
<b>Effects of Chiral Symmetry at μ<sub>B</sub>=0</b>	Di-lepton spectra at μ <sub>B</sub> =0	★ ■	Needs iTPC				HFT out		Enh
	Extended LPV observables	★ ■	Needs iTPC						Enh
<b>Internal Structure of the QGP and Color Response</b>	Y(1S,2S,3S)	○	✓						
	B R <sub>AA</sub>	★ ■	✓				✓		
	B v <sub>2</sub>	★ ■	✓				✓	✓	✓
	B-tagged Jets	○	✓				✓		
	Jets	○	✓						Enh
	γ -jets	○	✓					✓	
<b>Phase Diagram and Freeze-out</b>	BES-II Observables at μ <sub>B</sub> =0	★	Needs iTPC						
	C6/C2, C4/C2	★	Needs iTPC						
<b>The Strong Force</b>	Exotics and Bound States (di-Baryons)	★	Needs iTPC						✓
<b>Estimated Cost M\$</b>				2.0	4.0	0.6	5.0	1.0	4.5

✓ Measurement needs upgrade

Enh : Enhances measurement, but is not required

★ Unique to STAR    ○ Complementary to sPHENIX    ■ Complemented by LHC and/or JLab

Green highlighted rows require only continued running with STAR as instrumented for the BES-II

Base : STAR as instrumented for the BES-II

iTPC : Inner sector TPC upgrade extending coverage from |η|<1 to |η|<1.5

fTS : Forward Tracking System

fCal : Forward Electromagnetic and Hadronic Calorimeters

HFT+ : An extended faster heavy flavor tracker

Streaming : An electronics and DAQ upgrade allowing significant increase in minbias data rate

BSMD : Replacing the BSMD readout

HFT out: Di-lepton spectra at μ<sub>B</sub>=0 improved by running with less material

TABLE I: Summary of STAR's key physics goals in 2020+ and the upgrades needed to perform those measurements.

- 
- [1] L. Adamczyk et al. (STAR), Phys. Rev. Lett. **115**(9), 092002 (2015), 1405.5134
- [2] L. Adamczyk et al. (STAR), Phys. Rev. Lett. **113**, 072301 (2014), 1404.6880
- [3] J. Adams et al. (STAR), Phys. Rev. Lett. **92**, 171801 (2004), hep-ex/0310058
- [4] M.M. Mondal (STAR), PoS **DIS2014**, 216 (2014), 1407.3715
- [5] L. Adamczyk et al. (STAR) (2015), 1504.00415
- [6] J.L. Drachenberg (STAR), *Constraining Transversity and Nucleon Transverse-polarization Structure Through Polarized-proton Collisions at STAR*, in *Proceedings, 20th International Conference on Particles and Nuclei (PANIC 14)* (2014), pp. 181–184
- [7] K. Adkins (STAR), *Azimuthal Single-Spin Asymmetries of Charged Pions in Jets in  $\sqrt{s}=200$  GeV pp Collisions at STAR*, [http://indico.cern.ch/event/284740/session/34/contribution/55/attachments/526661/726219/KevinAdkins\\_spin2014.pdf](http://indico.cern.ch/event/284740/session/34/contribution/55/attachments/526661/726219/KevinAdkins_spin2014.pdf) (2015)
- [8] S. Fazio, D. Smirnov (STAR), PoS **DIS2014**, 237 (2014)
- [9] L. Song (STAR), *The Ridge and Di-hadron Correlations from the Beam Energy Scan at RHIC*, Presentation at QM2015 (2015)
- [10] S. Horvat (STAR), *Measurement of hadron suppression at 14.5 GeV and study of its connection with the disappearance of other QGP signatures at low  $\sqrt{s_{NN}}$  in Au+Au collisions with STAR at RHIC in BES I*, Presentation at QM2015 (2015)
- [11] J. Thaeder (STAR), *Higher moments of net-proton and net-charge multiplicity distributions at 14.5 GeV measured in Au+Au collisions at mid-rapidity with STAR at RHIC*, Presentation at QM2015 (2015)
- [12] G. Xie (STAR), *Nuclear Modification Factors of D Meson Production in Au+Au Collisions at  $\sqrt{s_{NN}} = 200$  GeV*, Presentation at QM2015 (2015)
- [13] M. Lomnitz (STAR), *Measurement of D Meson Azimuthal Anisotropy in Au+Au Collisions at  $\sqrt{s_{NN}} = 200$  GeV from STAR*, Presentation at QM2015 (2015)
- [14] R. Ma (STAR), *J/ $\Psi$  and  $\Upsilon$  measurements in the di-muon channel in Au+Au collisions at  $\sqrt{s_{NN}} = 200$  GeV with the STAR experiment*, Presentation at QM2015 (2015)
- [15] X. Li (STAR) (2015), 1506.06314
- [16] K. Kauder (STAR) (2015), 1509.08833
- [17] P. Jacobs (STAR), *Semi-inclusive charged jet measurements in Au+Au collisions at  $\sqrt{s_{NN}} = 200$  GeV with STAR*, Presentation at QM2015 (2015)
- [18] L. Adamczyk et al. (STAR), Phys. Rev. Lett. **112**(12), 122301 (2014), 1302.6184
- [19] N. Sahoo (STAR), *Direct-photon+hadron correlations to study parton energy loss with the STAR experiment*, Presentation at QM2015 (2015)
- [20] *RHIC Beam Projections*, <http://www.rhichome.bnl.gov/RHIC/Runs/RhicProjections.pdf> (2015)
- [21] *sPHENIX - An Upgrade Proposal from the PHENIX collaboration*, [http://www.phenix.bnl.gov/phenix/WWW/publish/documents/sPHENIX\\_proposal\\_19112014.pdf](http://www.phenix.bnl.gov/phenix/WWW/publish/documents/sPHENIX_proposal_19112014.pdf) (2014)
- [22] A. Airapetian et al. (HERMES), Phys. Lett. **B577**, 37 (2003), hep-ex/0307023
- [23] A. Airapetian et al. (HERMES), Phys. Lett. **B684**, 114 (2010), 0906.2478
- [24] D. de Florian, R. Sassot, Phys. Rev. **D69**, 074028 (2004), hep-ph/0311227
- [25] D. de Florian, R. Sassot, M. Stratmann, Phys. Rev. **D76**, 074033 (2007), 0707.1506
- [26] D. de Florian, R. Sassot, M. Stratmann, Phys. Rev. **D75**, 114010 (2007), hep-ph/0703242
- [27] T. Kaufmann, A. Mukherjee, W. Vogelsang (2015), 1506.01415
- [28] V. Khachatryan et al. (CMS), Phys. Rev. **D92**(1), 012003 (2015), 1503.08689
- [29] D. de Florian, S. Frixione, A. Signer, W. Vogelsang, Nucl. Phys. **B539**, 455 (1999), hep-ph/9808262
- [30] B. Surrus (STAR), PoS **DIS2014**, 241 (2014), 1407.4176
- [31] M. He, R.J. Fries, R. Rapp, Phys. Rev. **C86**, 014903 (2012), 1106.6006
- [32] S. Cao, G.Y. Qin, S.A. Bass, Phys. Rev. **C92**(2), 024907 (2015), 1505.01413
- [33] J. Xu, J. Liao, M. Gyulassy (2015), 1508.00552
- [34] A.M. Adare, M.P. McCumber, J.L. Nagle, P. Romatschke, Phys. Rev. **C90**(2), 024911 (2014), 1307.2188
- [35] T. Renk, Phys. Rev. **C88**(5), 054902 (2013), 1212.0646
- [36] H. Zhang, J.F. Owens, E. Wang, X.N. Wang, Phys. Rev. Lett. **103**, 032302 (2009), 0902.4000
- [37] K. Zapp, J. Stachel, U.A. Wiedemann, PoS **High-pT physics09**, 022 (2009), 0904.4885
- [38] A. Majumder, J. Putschke (2014), 1408.3403
- [39] F. D’Eramo, M. Lekaveckas, H. Liu, K. Rajagopal, JHEP **05**, 031 (2013), 1211.1922
- [40] M. Cacciari, G.P. Salam, G. Soyez, JHEP **04**, 063 (2008), 0802.1189
- [41] M. Cacciari, G.P. Salam, G. Soyez, Eur. Phys. J. **C72**, 1896 (2012), 1111.6097
- [42] B.I. Abelev et al. (STAR), Phys. Rev. **C82**, 034909 (2010), 0912.1871
- [43] L. Pang, Q. Wang, X.N. Wang, Phys. Rev. **C86**, 024911 (2012), 1205.5019
- [44] J. Jia, S. Radhakrishnan, M. Zhou (2015), 1506.03496
- [45] A. Bzdak, D. Teaney, Phys. Rev. **C87**(2), 024906 (2013), 1210.1965
- [46] A. Monnai, B. Schenke (2015), 1509.04103
- [47] A. Mazeliauskas, D. Teaney (2015), 1509.07492
- [48] R.S. Bhalerao, J.Y. Ollitrault, S. Pal, D. Teaney, Phys. Rev. Lett. **114**(15), 152301 (2015), 1410.7739

- [49] G. Aad et al. (ATLAS), ATLAS-CONF-2015-051 (2015)
- [50] V. Khachatryan et al. (CMS), Phys. Rev. **C92**(3), 034911 (2015), 1503.01692
- [51] G. Aad et al. (ATLAS), Phys. Rev. **C92**(3), 034903 (2015), 1504.01289
- [52] G. Aad et al. (ATLAS), Phys. Rev. **C90**(2), 024905 (2014), 1403.0489
- [53] P. Petreczky, C. Miao, A. Mocsy, Nucl. Phys. **A855**, 125 (2011), 1012.4433
- [54] O.D. Tsai et al., J. Phys. Conf. Ser. **587**(1), 012053 (2015)